

Article

Eco-Friendly Synthesis and Comparative In Vitro Biological Evaluation of Silver Nanoparticles Using *Tagetes erecta* Flower Extracts

Ana Flavia Burlec ^{1,†}, Monica Hăncianu ^{2,†}, Irina Macovei ¹, Cornelia Mircea ^{3,*} , Adrian Fifere ^{4,*},
Ioana-Andreea Turin-Moleavin ⁴, Cristina Tuchiluş ⁵, Silvia Robu ⁶ and Andreia Corciovă ¹ 

- ¹ Department of Drug Analysis, Faculty of Pharmacy, “Grigore T. Popa” University of Medicine and Pharmacy, 16 University Street, 700115 Iasi, Romania; ana-flavia.l.burlec@umfiasi.ro (A.F.B.); irina-macovei@umfiasi.ro (I.M.); acorciova@yahoo.com (A.C.)
- ² Department of Pharmacognosy, Faculty of Pharmacy, “Grigore T. Popa” University of Medicine and Pharmacy, 16 University Street, 700115 Iasi, Romania; mhancianu@yahoo.com
- ³ Department of Pharmaceutical Biochemistry and Clinical Laboratory, Faculty of Pharmacy, “Grigore T. Popa” University of Medicine and Pharmacy, 16 University Street, 700115 Iasi, Romania
- ⁴ Centre of Advanced Research in Bionanoconjugates and Biopolymers Department, “Petru Poni” Institute of Macromolecular Chemistry, 41A Grigore Ghica Voda Alley, 700487 Iasi, Romania; moleavin.ioana@icmpp.ro
- ⁵ Department of Microbiology, Faculty of Medicine, “Grigore T. Popa” University of Medicine and Pharmacy, 16 University Street, 700115 Iasi, Romania; cristina.tuchilus@umfiasi.ro
- ⁶ Department of Pharmacognosy, Faculty of Medicine and Pharmacy, “Dunarea de Jos” University, 35 Al. I. Cuza Street, 800010 Galati, Romania; silviarobu@yahoo.com
- * Correspondence: corneliimircea@yahoo.com (C.M.); fifere@icmpp.ro (A.F.)
- † These authors contributed equally to this work.



Citation: Burlec, A.F.; Hăncianu, M.; Macovei, I.; Mircea, C.; Fifere, A.; Turin-Moleavin, I.-A.; Tuchiluş, C.; Robu, S.; Corciovă, A. Eco-Friendly Synthesis and Comparative In Vitro Biological Evaluation of Silver Nanoparticles Using *Tagetes erecta* Flower Extracts. *Appl. Sci.* **2022**, *12*, 887. <https://doi.org/10.3390/app12020887>

Academic Editor: Adina Magdalena Musuc

Received: 20 December 2021

Accepted: 14 January 2022

Published: 16 January 2022

Publisher’s Note: MDPI stays neutral with regard to jurisdictional claims in published maps and institutional affiliations.



Copyright: © 2022 by the authors. Licensee MDPI, Basel, Switzerland. This article is an open access article distributed under the terms and conditions of the Creative Commons Attribution (CC BY) license (<https://creativecommons.org/licenses/by/4.0/>).

Abstract: The present study reports an eco-friendly synthesis method of silver nanoparticles (AgNPs) using two different extracts (aqueous and ethanolic) of *Tagetes erecta* flowers. When exposed to different biocompounds found in the plant, silver ions are reduced, thus, resulting in the green synthesis of nanoparticles. After performing the optimization of synthesis, the obtained AgNPs were characterized using various techniques. The UV–Vis spectrum of the synthesized nanoparticles showed maximum peaks at 410 and 420 nm. TEM analysis revealed that the particles were spherical with a size ranging from 10 to 15 nm, and EDX analysis confirmed the presence of silver metal. The average diameter value obtained through DLS analysis for the two types of AgNPs (obtained using aqueous and ethanolic extracts) was 104 and 123 nm. The Zeta potentials of the samples were -27.74 mV and -26.46 mV, respectively, which indicates the stability of the colloidal solution. The antioxidant and antimicrobial activities assays showed that nanoparticles obtained using the aqueous extract presented enhanced antioxidant activity compared to the corresponding extract, with both types of AgNPs exhibiting improved antifungal properties compared to the initial extracts.

Keywords: green synthesis; silver nanoparticles; marigold flowers; antioxidant; antifungal activity

1. Introduction

Nanoparticles are particles with dimensions in the 10^{-9} m range that possess special physico-chemical properties. These unique characteristics have recently led to increased attention regarding the research carried out on nanoparticles, as well as to the development of nanotechnology as an interdisciplinary field. Nanotechnology has applicability in many fields, being of great interest in medicine, pharmaceutical and cosmetics industries, energy, agriculture, environment, and food industry [1,2].

Silver nanoparticles (AgNPs), in particular, are known to have remarkable optical, electrical and antimicrobial properties. These properties can be correlated with the small particle size, and make it possible for AgNPs to be used in biosensors, composite fibers, superconducting materials, medical imaging, medicines, and cosmetics [3]. Out of all

biological properties, the antibacterial action is probably the most studied, as it offers new pharmacotherapeutic perspectives in the context of the rising resistance of pathogenic bacteria to classical antimicrobial agents [4]. Moreover, particularly important are the antioxidant and cytotoxic activities, that were more recently discovered for such materials, but are, nonetheless, more and more studied by researchers in the field [5,6].

The current study focuses on the importance of green chemistry in the synthesis of nanoparticles. Traditional physical and chemical methods are less and less used because they use toxic chemicals, require a large amount of energy, have high processing costs and generate nanoparticles with relatively low stability given their aggregation tendency [7]. Biological synthesis methods offer many advantages, which is why they are used preferentially instead of classical methods [8]. The main advantage is represented by the use of natural agents for the synthesis, stabilization and control of the shape, size and distribution of nanoparticles.

The present paper investigates the synthesis of silver nanoparticles using green chemistry and their characterization. For the synthesis of nanoparticles using biological methods, we chose *Tagetes erecta* (*T. erecta*), an ornamental plant very common in most geographical areas, taking into consideration its availability, as well as the fact that the species has been intensively studied regarding its chemical composition [9]. The species is a popular plant found in the Asteraceae family and it is widely cultivated for its decorative properties, as well as for the extraction of carotenoids [9,10]. It has been used since ancient times in traditional medicine, especially in Mexico and South America, to treat a wide variety of diseases and conditions. Moreover, the flowers of *T. erecta* are also found in the pages of the Mexican Pharmacopoeia [11].

In Mexico, the whole plant was used to make an infusion or a decoction in case of colds and respiratory disorders, but also to be used as a stimulant or as a muscle relaxant. Pressed juice or leaves were used as aphrodisiacs, diaphoretics, emetics, or for the treatment of liver disease or menstrual disorders. An ointment made from squeezing juice or leaves was applied externally in the treatment of malaria, to prevent the installation of chills. In Brazil, the infusion of the plant was intended for cases of bronchitis, cold, or rheumatism, while the infusion obtained from the roots was used as a laxative. In India, the juice obtained from flowers was administered internally to “purify” the blood, and the juice obtained from the whole plant was used as ear drops or as treatment for eye infections [11,12].

In the traditional medicine of various countries, it is believed that the flowers of the species can treat various skin infections, such as those that occur in case of wounds, burns, ulcers, eczema, or other dermatological conditions. The plant has also been used for kidney diseases, muscle or ear pain, or for the treatment of abscesses [13].

Taking into account the diversity of chemical compounds found in *T. erecta*, such as polyphenolic acids, flavonoids, carotenoids, terpenes, and thiophenes, it is easily understandable why a number of biological actions could be highlighted for different extracts obtained from this species, such as antioxidant, antimicrobial, antiproliferative, antidiabetic, and hepatoprotective [14–21]. Consequently, the species in question has an important pharmacological potential, given the multitude and diversity of effects observed during biological testing.

Therefore, the present study focused on the structural and morphological characterization of AgNPs obtained using aqueous and ethanolic extracts of *T. erecta* flowers in a comparative manner, as well as on their biological testing, especially considering their antioxidant and antimicrobial capacities. Few previous studies have synthesized different types of nanoparticles from the leaves, flowers, or other parts of this plant [22–26]. However, to the best of our knowledge, this is the first comparative study conducted on AgNPs synthesized using different types of *T. erecta* extracts.

2. Materials and Methods

2.1. Plant Material and Obtaining of Extracts

Tagetes erecta was cultivated in ecological conditions in North-Eastern Romania. The plant material (flowers) was dried in shade at a controlled temperature, until a constant mass. Two types of extracts were obtained using the flowers of the plant, through magnetic stirring. A total of 20 g of pulverized plant material was mixed using 200 mL solvent, which was either distilled water or ethanol. In both cases, the mixtures were blended using a magnetic stirrer for 30 min. Afterwards, the extracts were filtrated using a Whatman filter no. 1 and filled up to point with the same solvent. The 10% (*w/v*) liquid extracts were kept in a refrigerator at $-20\text{ }^{\circ}\text{C}$ until further use.

2.2. Green Synthesis of AgNPs

Aqueous solutions of silver nitrate (AgNO_3) of different concentrations were prepared for the synthesis of nanoparticles, which were eventually mixed with the two *T. erecta* extracts. The reaction conditions were varied in order to optimize the synthesis process, by varying the AgNO_3 solution concentration (1 mM, 3 mM, 5 mM, and 10 mM), the ratio between the volume of plant extract and that of AgNO_3 solution (1:9, 5:5, and 9:1), the pH (2, 5, and 8), the temperature of the synthesis ($20\text{ }^{\circ}\text{C}$, $40\text{ }^{\circ}\text{C}$, $60\text{ }^{\circ}\text{C}$, and $80\text{ }^{\circ}\text{C}$), and the stirring time (0, 15, 30, 45, 60, and 75 min).

After establishing the reaction conditions, the colloidal solutions were centrifuged at 10,000 rpm for 30 min. For the purification of nanoparticles, the supernatant was removed and the AgNPs were redispersed in distilled water, centrifuged, and finally separated. This operation was repeated twice, and the obtained AgNPs were dried in an oven at a temperature of $40\text{ }^{\circ}\text{C}$, until a constant mass. The synthesized samples were kept at $4\text{ }^{\circ}\text{C}$ and were assigned the following codes: AgNPs-H₂O for the AgNPs obtained using the aqueous extract of *T. erecta* flowers, and AgNPs-EtOH for those obtained using the ethanolic extract.

2.3. Characterization of the Synthesized AgNPs

The formation of AgNPs was observed through the color change of *T. erecta* extracts after being mixed with AgNO_3 . The synthesized AgNPs were characterized using UV-visible spectroscopy, with the UV-Vis spectra being recorded in the 250–600 nm range to distinguish the maximum surface plasmon resonance (SPR). For this determination, a Jasco V-530 UV-Vis double beam spectrophotometer (Jasco, Tokyo, Japan) was used.

In order to investigate the different functional groups of the extract and those involved in the AgNPs synthesis, the FTIR spectra of both extracts and AgNPs were recorded using a Vertex 70 Spectrometer (Bruker, Billerica, MA, USA) by potassium bromide tableting, in a scan interval of $4000\text{--}310\text{ cm}^{-1}$.

EDX qualitative analysis was performed using a Quanta 200 Environmental Scanning Electron Microscope (ESEM) with EDX (FEI Company, Brno, Czech Republic). The employed detector allowed rapid determination of the elemental composition of the biosynthesized nanoparticles.

The DLS analysis was carried out using a Delsa Nano Submicron Particle Size Analyzer (Beckman Coulter Inc., Fullerton, CA, USA), that measured the average diameter of AgNPs and the Zeta potential. Additionally, the morphology and dimensions of nanoparticles were investigated by TEM analysis, which was performed using a High-Tech HT 7700 Transmission Electron Microscope (Hitachi High-Technologies Corporation, Tokyo, Japan).

Furthermore, prior to the purification of AgNPs, the plant extract and the corresponding supernatant were evaluated regarding the total phenolic content using a modified spectrophotometric Folin-Ciocalteu method [27]. The standard was represented by gallic acid. The tests were performed in triplicate and the results were expressed in mg gallic acid equivalents (GAE)/mL sample.

2.4. In Vitro Antioxidant Activity

The following in vitro tests were used to study the antioxidant activity of the samples: inhibition of erythrocyte hemolysis mediated by peroxy free radicals and 15-lipoxygenase (LOX) inhibition.

The inhibition of erythrocyte hemolysis was determined using a method proposed by Barros et al. [28]. Over 0.7 mL sample solution prepared in dimethyl sulfoxide, 0.2 mL of 100 mM 2,2'-azobis-(2-amidinopropane) dihydrochloride solution in phosphate buffer pH 7.4, and 0.1 mL of 10% erythrocyte suspension in 0.9% saline solution were added. The mixture was kept at 37 °C for 3 h, after which it was brought at room temperature, diluted with 3 mL phosphate buffer pH 7.4, and centrifuged at 3000 rpm for 10 min. The absorbance of the sample solution (A_P) was then read at 540 nm using a control prepared under the same conditions, but without adding erythrocyte suspension. The positive control was represented by a 2,2'-azobis-(2-amidinopropane) dihydrochloride in 100 mM phosphate buffer solution and 10% erythrocyte suspension and its absorbance was also determined at 540 nm (A_{AAPH}). The ability to inhibit peroxy radical-mediated hemolysis was calculated according to the formula: Inhibition (%) = $100 \times (A_{AAPH} - A_P) / A_{AAPH}$. All experiments were performed in triplicate and gallic acid was used as positive control.

The 15-LOX inhibition capacity of extracts and of their corresponding AgNPs was evaluated using the modified Malterud method [9,29]. In total, 50 µL lipoxidase from *Glycine max* in borate buffer (pH 9) and 50 µL of the sample/control solution were mixed and then left to stand for 10 min. Then, 2 mL 0.16 mM linoleic acid borate buffer were added, and the absorbance was recorded at 234 nm for 90 s. The inhibitory activity was calculated using the formula: Inhibition (%) = $(A_{FI} - A_{CI}) \times 100 / A_{FI}$, where A_{FI} is the difference between the absorbances of the enzyme solution without inhibitor at 90 and 30 s, while A_{CI} is the difference between the enzyme-inhibitor solution absorbances at 90 and 30 s. Gallic acid was used as positive control. All experiments were performed in triplicate.

2.5. Antimicrobial Activity

The antimicrobial activity was evaluated by means of a disk diffusion method, using Mueller–Hinton agar (Biolab) for fungi and Mueller–Hinton agar (Oxoid) for bacteria. The tested microorganisms, available in from the Culture Collection of the Department of Microbiology, “Grigore T. Popa” University of Medicine and Pharmacy, Iași, Romania, were: *Staphylococcus aureus* (*S. aureus*) ATCC 25923, *Pseudomonas aeruginosa* (*P. aeruginosa*) ATCC 27853, and *Candida albicans* (*C. albicans*) ATCC 90028. After applying the samples (extracts and AgNPs) on the agar found in Petri plates, followed by their incubation for 24 h at 35 °C, the inhibition zones were measured [30,31]. Discs containing ciprofloxacin (5 µg/disc) and fluconazole (25 µg/disc) were used as positive controls. All experiments were performed in triplicate and the results were expressed as mean ± standard deviation.

3. Results

3.1. AgNPs Synthesis

The synthesis of AgNPs with the use of plant extracts generally involves the obtaining of extracts and silver salt solutions, formation of the AgNPs by mixing the two solutions in different amounts and under certain medium conditions (pH, stirring time, and temperature), steps that were also applied in our case. The final phase was represented by the separation and purification of nanoparticles, followed by the confirmation of AgNPs synthesis through different analytical approaches.

Firstly, the formation of AgNPs was observed, taking into account the color change. After the reaction was completed, a change in color from yellow to brown was observed, which, according to other studies, can be attributed to the reduction of Ag^+ to metal nanosilver, Ag^0 [32,33].

The successful synthesis of AgNPs was afterwards confirmed by SPR detection via UV-Vis spectrophotometry in the 400 to 500 nm range [34,35]. Furthermore, these optical features have been used for the analysis of optimal synthesis conditions.

3.2. Optimization of AgNPs Synthesis

3.2.1. The Influence of Silver Nitrate Concentration on AgNPs Synthesis

This parameter was measured by varying AgNO_3 concentrations, with four different values (1 mM, 3 mM, 5 mM, and 10 mM) being investigated for the formation of nanoparticles using *T. erecta* aqueous extract. Therefore, four samples containing 1 mL of extract brought to a pH value of 8 using 0.1 M NaOH were treated with 9 mL AgNO_3 solution of one of the following concentrations: 1 mM, 3 mM, 5 mM, and 10 mM, respectively.

The initial spectrum of each mixture was recorded. After further mixing of samples with AgNO_3 solutions using a magnetic stirrer for one hour, the final spectra were recorded (Figure 1).

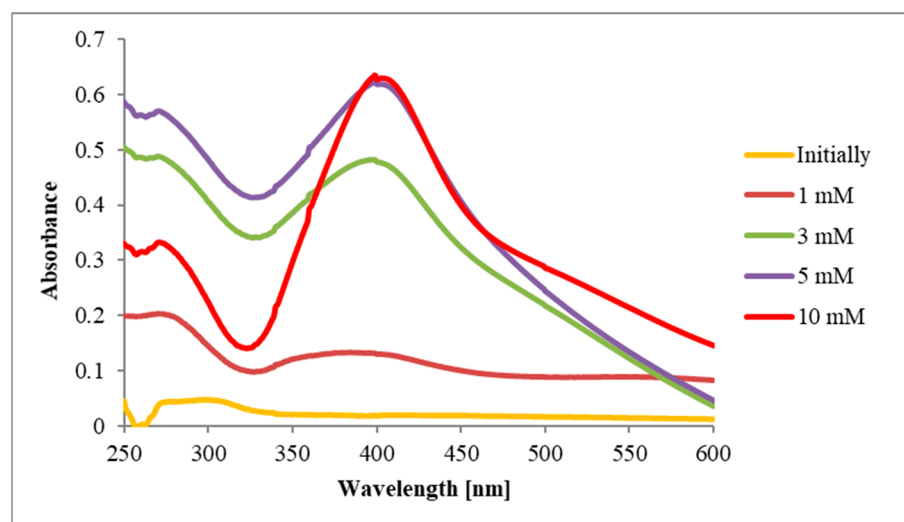


Figure 1. The influence of different AgNO_3 concentrations (1 mM, 3 mM, 5 mM, and 10 mM) on AgNPs- H_2O formation.

It can be observed that with the increase of AgNO_3 concentration, the quantity of obtained nanoparticles increases as well. However, the 3 mM value was chosen as the optimal concentration, given that it is the lowest concentration at which the peak specific to the synthesized AgNPs appears.

On the other hand, when recording the absorption spectra for the four samples in case of AgNPs-EtOH (Figure 2), similar values of the maximum absorbances for the samples containing 1 mM, 3 mM, and 5 mM AgNO_3 solution were observed, but the lowest concentration (1 mM) was chosen as the optimal concentration for the nanoparticles' formation.

3.2.2. The Influence of Plant Extract: AgNO_3 Ratios on AgNPs synthesis

In order to determine the optimal ratio for AgNPs- H_2O formation, three variations of the ratio between the *T. erecta* extract and the AgNO_3 solution (1:9, 5:5 and 9:1) were tested.

For the first sample, 1 mL of extract was brought to a pH of 8 using a 0.1 M NaOH solution, then 9 mL of 3 mM AgNO_3 was added. For the second sample, 5 mL of extract was brought to a pH of 8 and 5 mL of 3 mM AgNO_3 were added, while for the last sample, 9 mL of extract was brought to a pH of 8 and 1 mL of 3 mM AgNO_3 was eventually added. The three samples were left under magnetic stirring for one hour and then the absorption spectra were recorded (Figure 3).

The characteristic peak for AgNPs formation appeared at 410 nm for the 1:9 plant extract: AgNO_3 ratio, which was further used for the proper synthesis.

For AgNPs-EtOH formation, the same procedure was used for the samples. After one hour of magnetic stirring, the absorption spectra were recorded (Figure 4).

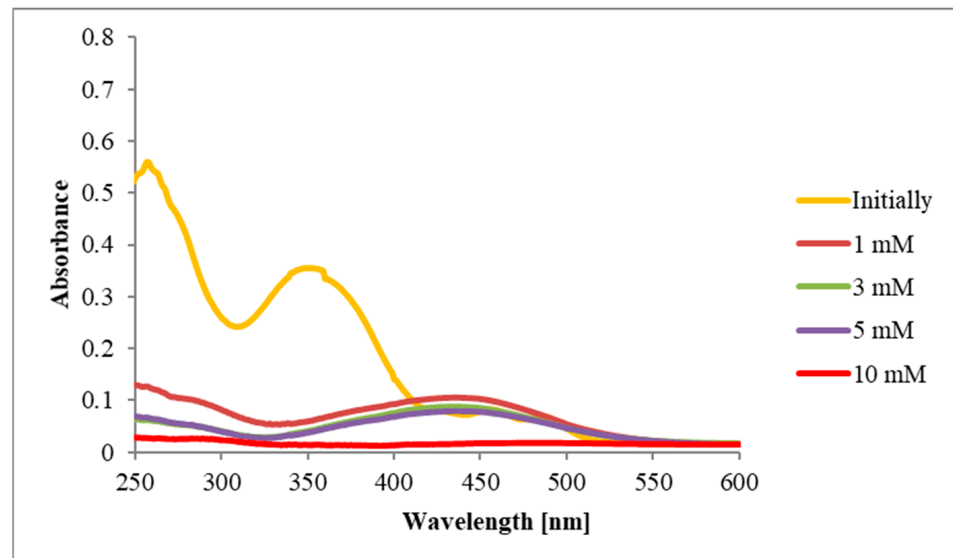


Figure 2. The influence of different AgNO_3 concentrations (1 mM, 3 mM, 5 mM, and 10 mM) on AgNPs-EtOH formation.

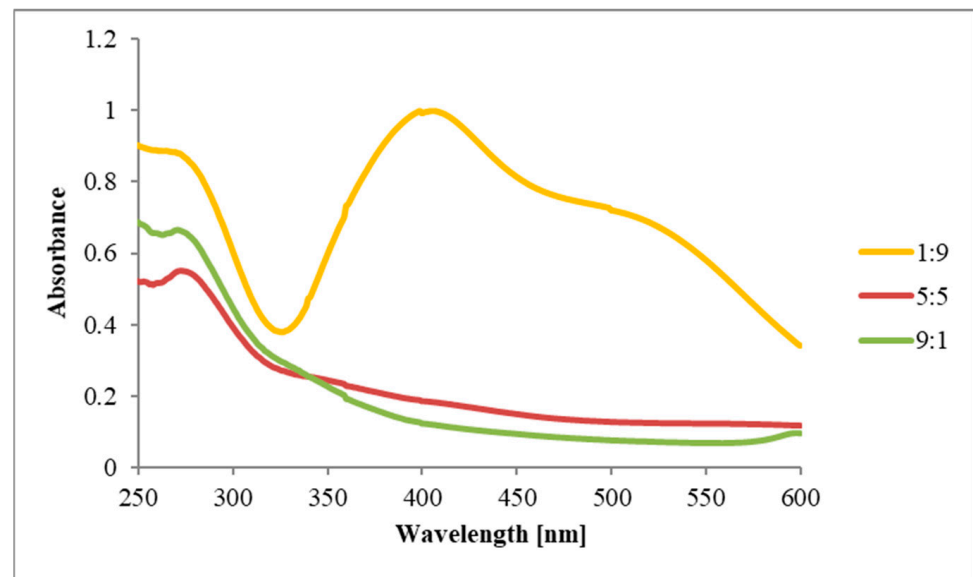


Figure 3. The influence of different plant extract: AgNO_3 ratios (1:9, 5:5 and 9:1) on AgNPs- H_2O formation.

Out of the three investigated variations of the volume ratios, the peak corresponding to the formation of AgNPs-EtOH formation was more conclusive in the case of the 5:5 plant extract: AgNO_3 ratio.

3.2.3. The Influence of pH on AgNPs Synthesis

The initial pH of the *T. erecta* aqueous extract was determined, with the obtained value being 5. In order to determine the optimum pH required for the reactions between the components of the extract and the silver nitrate solution, 1 mL of extract was taken and adjusted to a pH value of 2 using a solution of 0.1 M HCl, and to a pH of 8 with a 0.1 M NaOH solution. Then, 1 mL of the extract was added to another vial without changing its

pH. A total of 9 mL of 3 mM AgNO_3 were added, the mixtures were stirred for one hour, then the absorption spectra for each of the three mixtures, corresponding to pH values of 2, 5, and 8, were recorded. The UV-Vis spectra obtained for the three samples are presented in Figure 5.

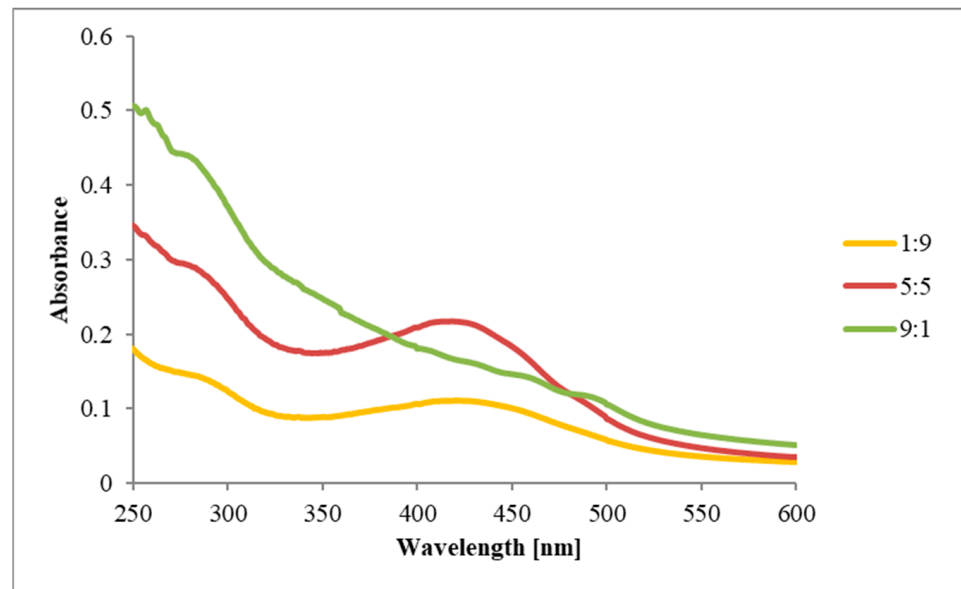


Figure 4. The influence of different plant extract: AgNO_3 ratios (1:9, 5:5 and 9:1) on AgNPs-EtOH formation.

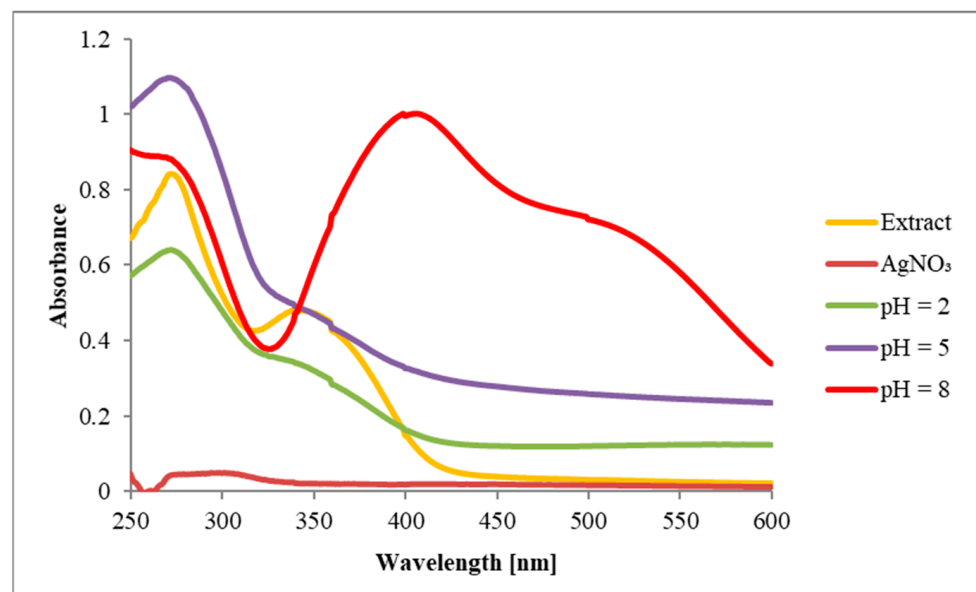


Figure 5. The influence of pH (2, 5, and 8) on AgNPs- H_2O formation.

The spectra show that at pH 2 and 5, AgNPs synthesis is suppressed. On the other hand, at pH 8, a well-r demonstrating the formation of AgNPs- H_2O . It should be noted that, in the 400–500 nm range, the spectra of the AgNO_3 solution and of the plant extract do not display peaks. Therefore, the extract brought to a pH of 8 was further used for the actual synthesis.

Considering the three samples with different pH values, and after recording their corresponding spectra, it was observed that in this case as well, the pH value at which the peak corresponding to the formation of AgNPs was obtained (420 nm) was also 8 (Figure 6).

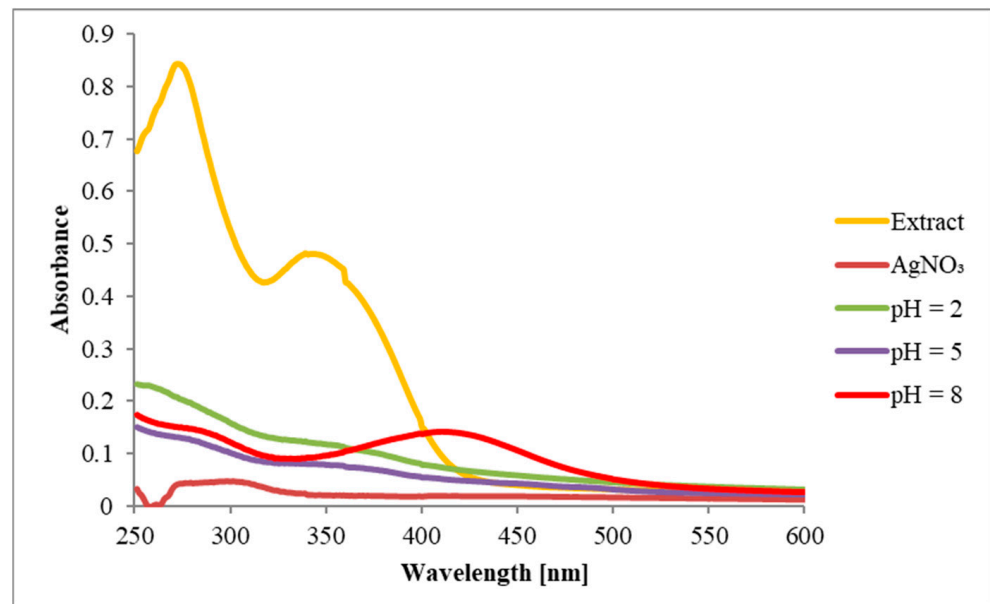


Figure 6. The influence of pH (2, 5, and 8) on AgNPs-EtOH formation.

3.2.4. The Influence of Temperature on AgNPs Synthesis

In order to optimize even further the reaction conditions, the samples with the reaction mixture consisting of *T. erecta* extract brought to a pH of 8 and of 3 mM AgNO₃ solution (1:9 ratio) were stirred for one hour at different temperatures: 20 °C, 40 °C, 60 °C, and 80 °C, respectively. The absorption spectra recorded for the four samples are presented in Figure 7.

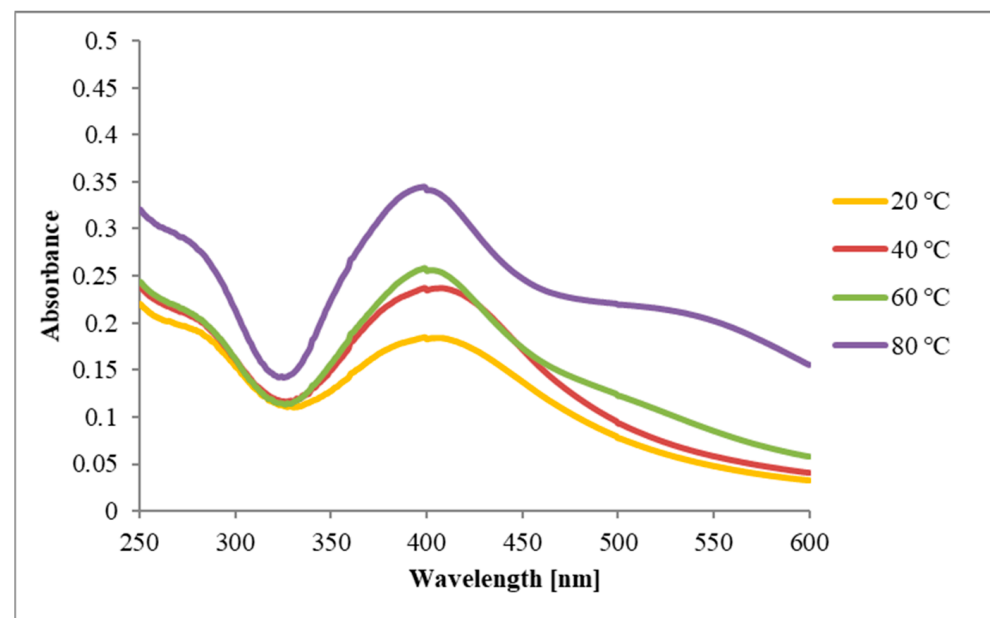


Figure 7. The influence of temperature (20 °C, 40 °C, 60 °C, and 80 °C) on AgNPs-H₂O formation.

The measured absorbance increases with temperature, reaching the highest value of absorbance at 80 °C. However, given that satisfactory results were obtained at 40 °C, that this temperature is easier to reach, and that the temperature is low enough that the active components of the plant extract do not deteriorate excessively, this value was chosen as the optimal one for the AgNPs-H₂O synthesis.

Regarding AgNPs-EtOH formation, an increase in absorbance was observed on the recorded absorption spectra, which is directly proportional to the temperature increase and a maximum absorbance was obtained when the sample was heated up to 80 °C. However, given the same considerations as in the first case, the temperature of 40 °C was chosen for the actual AgNPs synthesis (Figure 8).

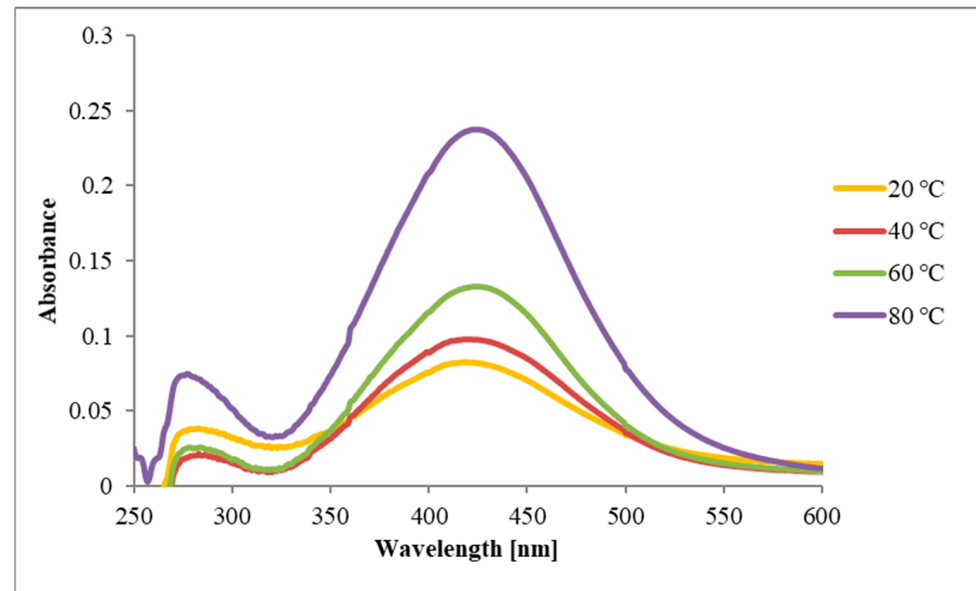


Figure 8. The influence of temperature (20 °C, 40 °C, 60 °C, and 80 °C) on AgNPs-EtOH formation.

3.2.5. The Influence of Stirring Time on AgNPs Synthesis

In order to complete the optimal synthesis conditions, the reaction was monitored during stirring every 15 min for 75 min. A total of 3 mL of the extract was brought to a pH of 8 using a 0.1 M NaOH solution, 27 mL of 3 mM AgNO₃ solution was added, after which a first spectrum was recorded (0 min). The samples were stirred magnetically, and a small volume was collected every 15 min to record a new spectrum. The corresponding spectra at 0, 15', 30', 45', 60', and 75' are presented in Figure 9.

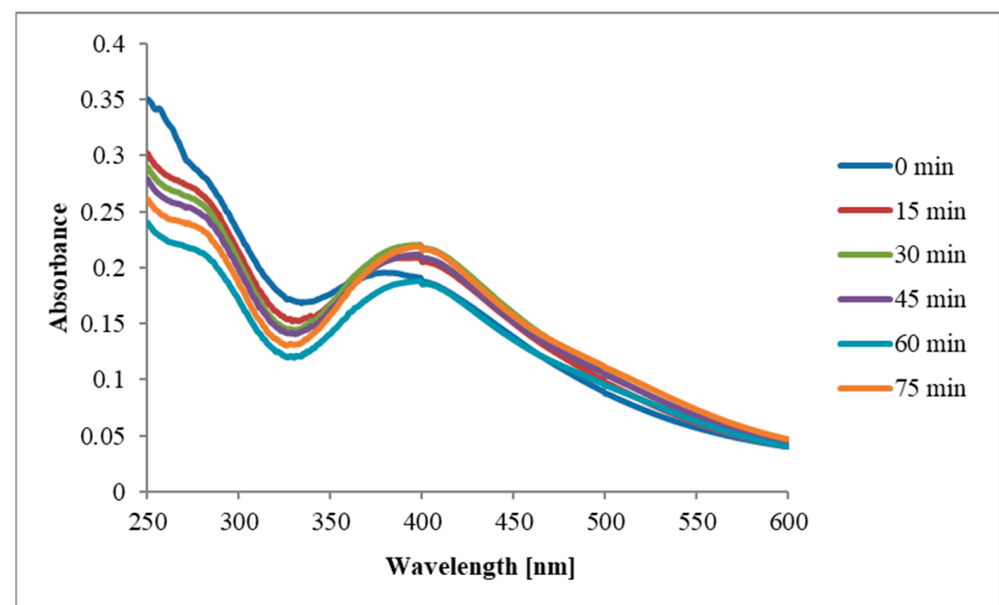


Figure 9. The influence of stirring time (0, 15', 30', 45', 60', and 75') on AgNPs-H₂O formation.

The reaction began almost immediately, with the peak corresponding to AgNPs formation being observed even after the first 15 min. As the stirring time increased, so did the absorbance, which proves that the concentration of the obtained AgNPs increases with stirring time. The same is true for AgNPs obtained using *T. erecta* ethanolic extract (Figure 10).

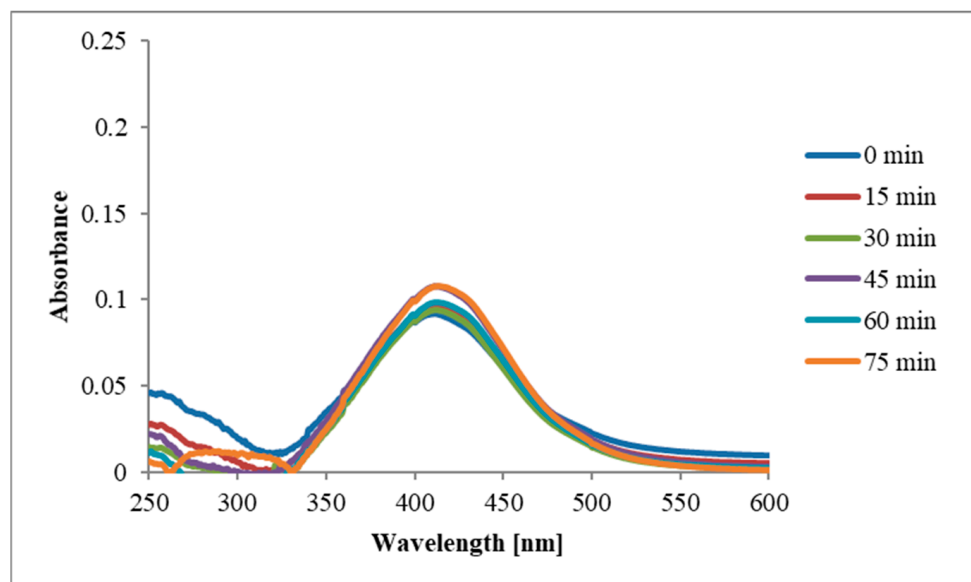


Figure 10. The influence of stirring time (0, 15', 30', 45', 60', and 75') on AgNPs-EtOH formation.

3.3. Characterization of The Synthesized AgNPs

3.3.1. Visual Inspection

The monitoring of AgNPs synthesis can be performed primarily by observing the color change of the reaction mixture (extract and AgNO_3) [36]. For both the ethanolic extract and the aqueous extract, a change in color was observed after mixing with the 3 mM AgNO_3 solution. Even if the mixture was initially yellow, over time the color changed to brown and eventually to dark brown, due to the effect of surface plasmon resonance.

3.3.2. Fourier Transform Infrared Spectroscopy (FTIR) Analysis

FTIR analysis of the extracts and their derived AgNPs was performed in order to investigate the functional groups of the possible phytoconstituents involved in nanoparticles' biosynthesis and stabilization. The FTIR spectra of extracts and of their derived AgNPs are depicted in Figure 11.

Both aqueous and ethanolic extracts of *T. erecta* show strong absorption bands at 3424 cm^{-1} and 3406 cm^{-1} corresponding to the stretching vibration of O-H groups in alcohols and phenols. Bands at 2922 cm^{-1} and 2853 cm^{-1} for *T. erecta* extracts are assigned to N-H bonds in amides and C-H stretching vibrations, respectively. Common intense bands for both extracts present at 1622 cm^{-1} and 1072 cm^{-1} denote C=O and C-O-C stretching vibrations, respectively.

Stretching vibrations of the aromatic ring and phenyl groups were also identified through the absorption bands at 792 cm^{-1} , 619 cm^{-1} (aqueous extract) and 818 cm^{-1} , 610 cm^{-1} (ethanolic extract).

3.3.3. Transmission Electron Microscopy (TEM) Analysis

The morphology, shape and size of AgNPs were determined using TEM, the recorded images being shown in Figure 12.

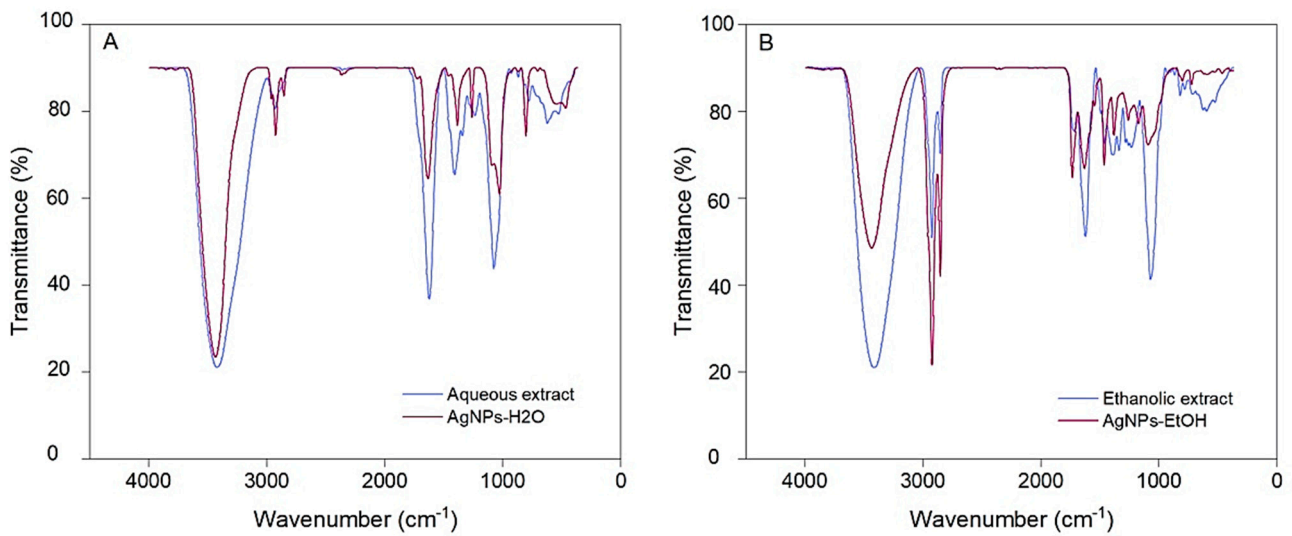


Figure 11. Comparative FTIR spectra of initial extracts and of their derived nanoparticles: AgNPs-H₂O (A) and AgNPs-EtOH (B).

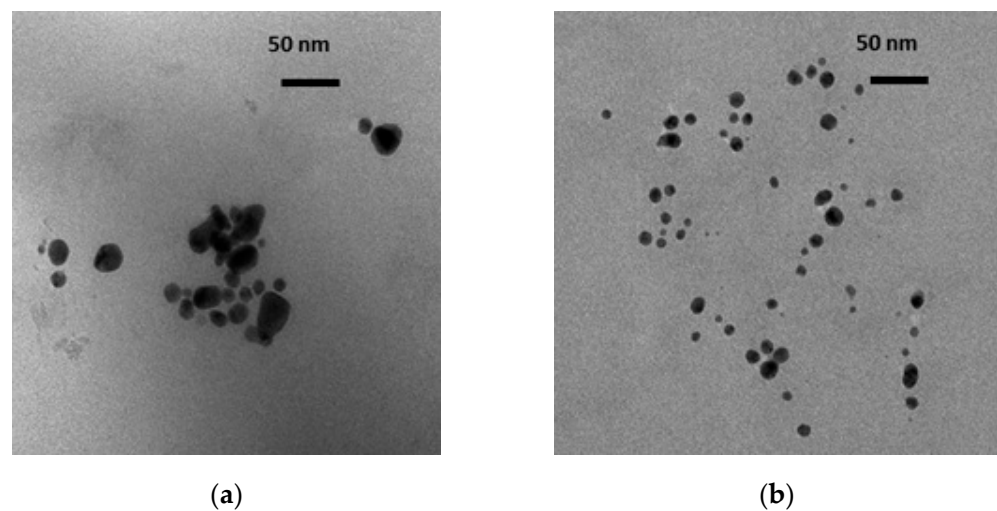


Figure 12. TEM images of AgNPs-H₂O (a) and of AgNPs-EtOH (b).

TEM images show well-individualized nanoparticles of almost spherical shape, more pronounced in the case of AgNPs-EtOH. AgNPs-H₂O presented an average diameter of approximately 15 nm, while AgNPs-EtOH of around 10 nm.

The average size of AgNPs synthesized using *T. erecta* flowers under the previously mentioned conditions was smaller than those presented in other papers. For example, Dhuldhaj et al. described AgNPs obtained using an aqueous extract of *T. erecta* leaves as spherical and polydisperse, with an average diameter of 30 nm [24]. Similarly, for an aqueous extract of *T. erecta* leaves, Tyagi et al. obtained mostly spherical AgNPs with an average size of 22 nm [37].

3.3.4. Energy Dispersive X-ray (EDX) Analysis

For highlighting the presence of silver, the EDX spectra of the obtained nanoparticles were recorded and can be found in Figure 13.

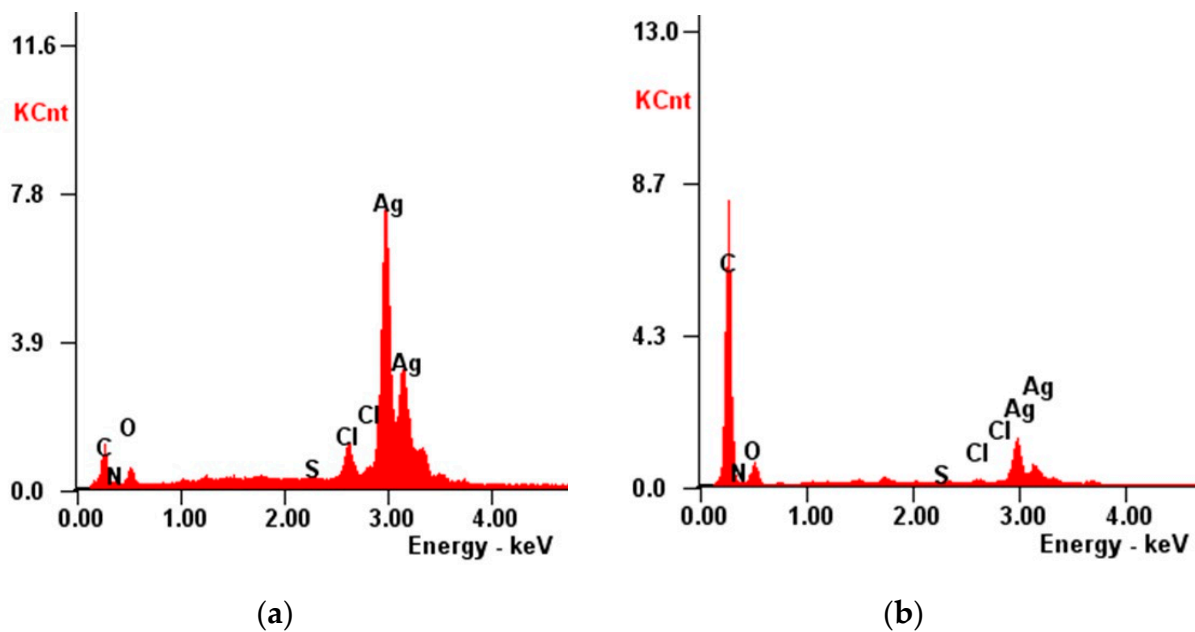


Figure 13. EDX spectra of AgNPs-H₂O (a) and of AgNPs-EtOH (b).

The elemental composition of the synthesized AgNPs analyzed by EDX showed in both cases the signal peak at 3 keV corresponding to Ag, but also signals corresponding to other elements, mainly to C, O, and N.

For the two samples taken into study, the proportions in which the elements can be found is different. Consequently, for AgNPs-H₂O, the following proportions were observed: Ag—77.23%, C—10.35%, O—6.59%, and N—1.32%; while for AgNPs-EtOH, Ag represents 13.4%, C—69.81%, O—10.84%, and N—5.57%.

3.3.5. DLS Characterization and Zeta Potential Determination

DLS analysis was used to determine the electrical charge of the surface (Figure 14) and the hydrodynamic diameter of AgNPs.

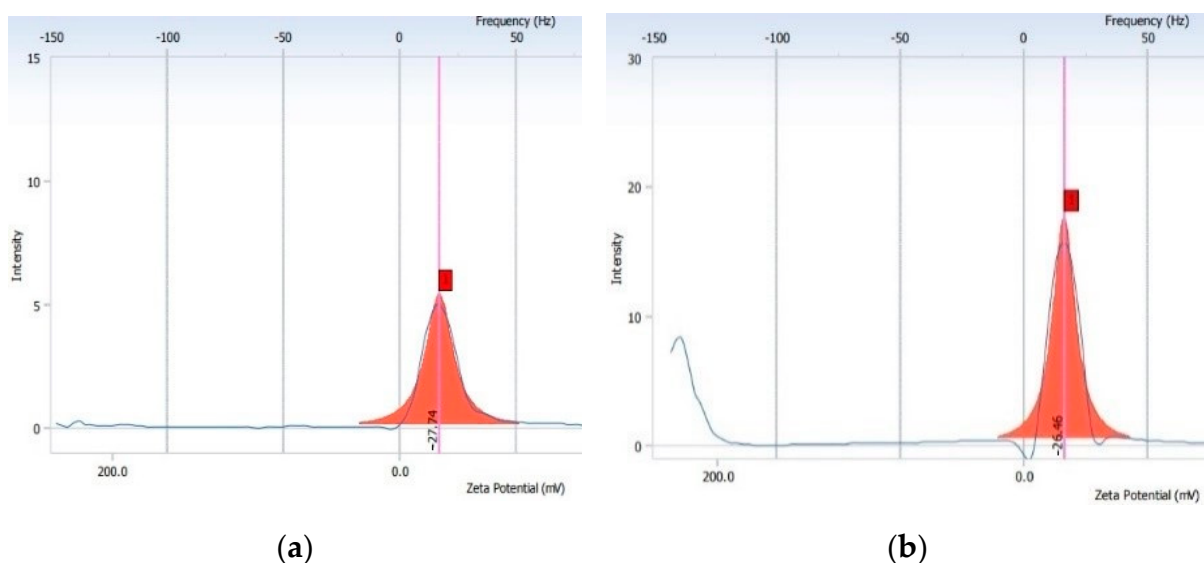


Figure 14. Zeta potential of AgNPs-H₂O (a) and of AgNPs-EtOH (b).

The average diameter value obtained for AgNPs-H₂O was 104 nm, while for AgNPs-EtOH the hydrodynamic diameter was 123 nm. The Zeta potential of AgNPs-H₂O was −27.74 mV, while for AgNPs-EtOH the obtained value was −26.46 mV.

A Zeta potential value of ± 30 mV is believed to indicate the existence of a stable suspension [23].

3.3.6. Evaluation of The Total Phenolic Content of Extracts Used for AgNPs Synthesis

Taking into consideration that biomolecules such as polyphenols from the extract participate in AgNPs synthesis, the content in phenolic compounds found in the initial extracts and in the supernatant obtained after separation of nanoparticles was determined. The results are summarized in Table 1.

Table 1. Content in phenolic compounds of the plant extract and of the supernatant obtained after AgNPs separation.

Sample	Content in Phenolic Compounds (mg GAE/mL Sample)	
	Plant Extract	Supernatant after Separation of AgNPs
AgNPs-H ₂ O	0.1050 \pm 0.002	0.0671 \pm 0.003
AgNPs-EtOH	0.2267 \pm 0.001	0.1960 \pm 0.004

Judging by the data found in Table 1, the amount of phenolic compounds that can be found in the plant extract is higher than that found in the supernatant obtained after separation of AgNPs, which indicates a loss of such compounds in the synthesis process, corresponding to the attachment of these compounds on the outer layer of AgNPs. To the best of our knowledge, this is the first report on such a determination carried out on both the initial *T. erecta* extract, as well as on the supernatant.

3.4. In Vitro Evaluation of the Antioxidant Activity

Antioxidant compounds block peroxy radical synthesis induced by 2,2'-azobis- (2-amidinopropane) dihydrochloride, protecting the erythrocyte membrane. By reducing the concentration of peroxy radicals, the absorbance of the solution measured at 540 nm is also reduced. The degree of inhibition of erythrocyte hemolysis by the samples and gallic acid is presented in Figure 15.

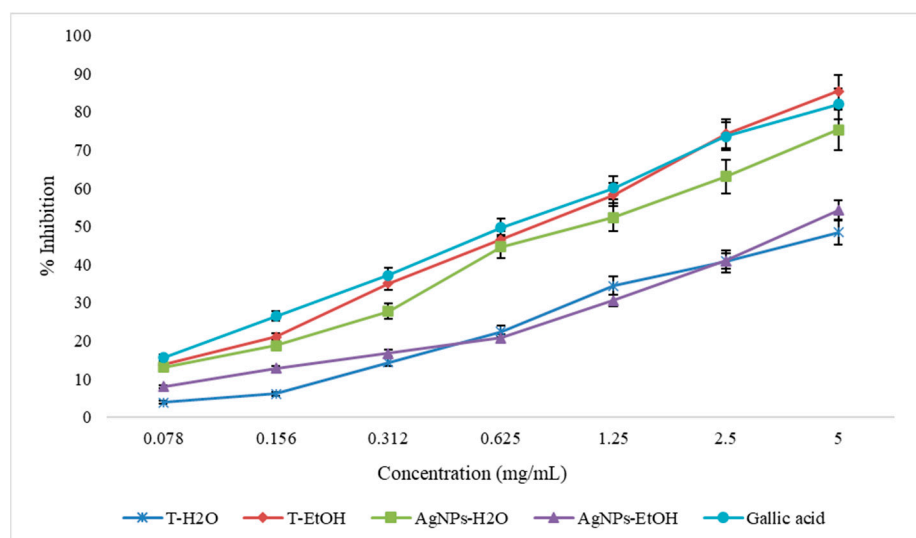


Figure 15. Graphical representation of the erythrocyte hemolysis inhibition capacity (%) of extracts and of their corresponding AgNPs solutions, compared to gallic acid.

Taking into consideration that bioactive compounds could inhibit the 15-LOX enzyme by blocking the oxidation of linoleic acid, the enzyme inhibition capacity of samples was assessed. The results obtained for the extracts and for their corresponding AgNPs during this assay can be seen in Figure 16.

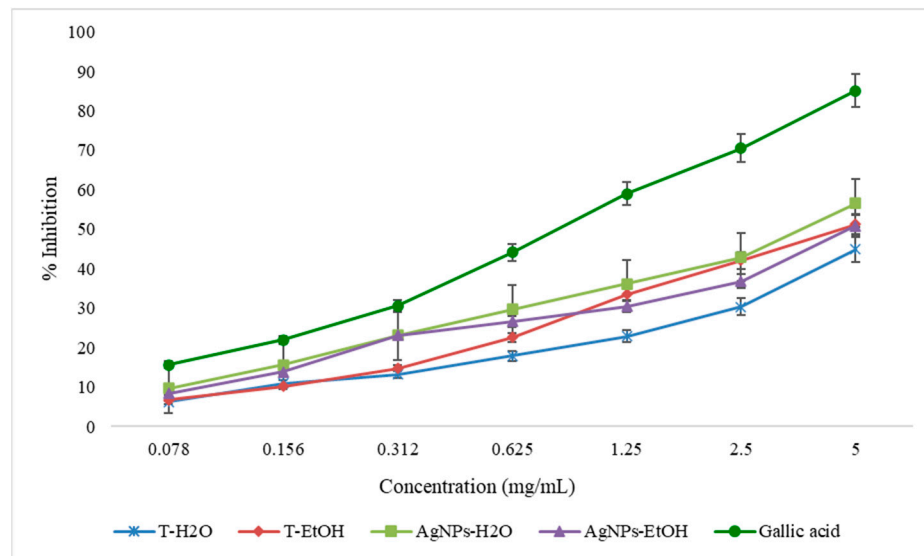


Figure 16. Graphical representation of the 15-LOX inhibition capacity (%) of extracts and of their corresponding AgNPs solutions, compared to gallic acid.

The EC_{50} values of the extracts and of the synthesized nanoparticles obtained during the two antioxidant determinations are presented in Table 2. The EC_{50} values are inversely proportional with the efficacy of the antioxidant activity.

Table 2. EC_{50} values of *T. erecta* extracts and of their corresponding AgNPs obtained in the antioxidant assays.

Sample	EC_{50} ($\mu\text{g/mL}$ Final Solution)	
	Inhibition of Erythrocyte Hemolysis	15-LOX Inhibition
Aqueous extract	-	-
Ethanollic extract	53.62 ± 1.96	75.89 ± 6.06
AgNPs-H ₂ O	70.83 ± 1.10	59.66 ± 2.39
AgNPs-EtOH	280.86 ± 0.89	79.72 ± 3.49
Gallic acid	44.83 ± 0.49	13.68 ± 0.88

As it can be seen in the case of AgNPs obtained using *T. erecta* aqueous extract, the antioxidant activity tested through the inhibition of erythrocyte hemolysis increases and the EC_{50} could be measured in the tested concentration range ($70.83 \pm 1.10 \mu\text{g/mL}$ final solution), unlike that of the corresponding extract. The same is true for the lipoxygenase inhibition assay, in which the EC_{50} value of AgNPs-H₂O was shown to be $59.66 \pm 2.39 \mu\text{g/mL}$ final solution. However, in both antioxidant assays, the ethanolic extract presented a more promising activity than that of the corresponding AgNPs.

3.5. Antimicrobial Activity

The antimicrobial activity of the plant extracts and of their derived AgNPs was tested against three pathogenic microbial strains: a Gram-positive bacterium (*Staphylococcus aureus*), a Gram-negative bacterium (*Pseudomonas aeruginosa*), and a fungal strain (*Candida albicans*). The results are presented in Table 3 as mean value of the inhibition zone (measured in mm) \pm standard deviation.

Table 3. Antimicrobial activity of the plant extracts and of the corresponding AgNPs.

Samples/Standards	Diameter of Inhibition Zones (mm) \pm SD		
	<i>Staphylococcus aureus</i> ATCC 25923	<i>Pseudomonas aeruginosa</i> ATCC 27853	<i>Candida albicans</i> ATCC 90028
Aqueous extract	14.0 \pm 0.00	NA *	13.0 \pm 0.00
Ethanol extract	14.0 \pm 0.00	NA *	12.0 \pm 0.00
AgNPs-H ₂ O	14.0 \pm 0.00	NA *	14.0 \pm 0.00
AgNPs-EtOH	14.0 \pm 0.00	NA *	20.0 \pm 0.00
Ciprofloxacin	30.0 \pm 0.00	30.3 \pm 0.57	* NT
Fluconazole	NT *	NT **	29.0 \pm 0.00

* NA—no activity detected; ** NT—not tested.

The most promising activity on *C. albicans* of the tested AgNPs in comparison to their corresponding extract was observed for AgNPs-EtOH, with a diameter of the inhibition zone almost double than that of the initial extract (20.0 \pm 0.00, compared to 12.0 \pm 0.00 mm), which illustrates the improved antifungal action of the biosynthesized nanoparticles.

Regarding the testing on *S. aureus*, it can be noticed that the investigated extracts and nanoparticles show a degree of bacterial inhibition capacity (14.0 \pm 0.00 mm), with no variations between the extracts and the corresponding AgNPs. No activity was detected for any of the tested samples on the Gram-negative bacteria.

4. Discussion

The mechanism surrounding the green synthesis of AgNPs using plants usually involves the preparation of nanoparticles by mixing the plant extract and silver salt solutions in different proportions, for different stirring times and at certain pH and temperature values. When exposed to plant compounds, Ag⁺ is reduced to Ag⁰, followed by the formation of oligomeric clusters and AgNPs synthesis [38]. Thus, silver ions suffer a bioreduction process that is believed to be due to biomolecules found in plant extracts (e.g., polyphenols, flavonoids, polysaccharides), being eventually transformed into colloidal silver which will form aggregates. Such aggregates will eventually stabilize through the attachment of biocompounds from the medium to their surface [35,39]. The decrease in the content of phenolic compounds found in the supernatant obtained after separation of AgNPs compared to that of the initial extract indicates the importance such polyphenols play in the synthesis of nanoparticles.

The optimization of the synthesis demonstrated that, in the case of *T. erecta* aqueous extract, the most suitable reaction conditions for AgNPs obtaining were: pH 8, 3 mM AgNO₃ solution, extract:AgNO₃ ratio of 1:9, 40 °C temperature, and stirring time of 75 min. In the case of the ethanolic extract, the most suitable reaction conditions for obtaining AgNPs were similar, the only difference being noticed regarding the optimal extract: AgNO₃ volume ratio which was 5:5 in the latter case.

Regarding FTIR analysis, absorption bands in extracts were also visible in their derived AgNPs spectra, in some cases being attenuated or shifted, suggesting the attachment of functional groups from the extract compounds to the nanoparticles' surface. IR spectra of the extracts and their derived AgNPs indicate that polyphenols and flavonoids are the major compounds involved in the biosynthesis of nanoparticles, having also a role as capping agents [40,41].

The EDX analysis showed a dominant peak at 3 KeV, that is typical for AgNPs, and demonstrates the presence of silver in the synthesized nanoparticles and, implicitly, of the SPR band. In the case of AgNPs-H₂O, a stronger signal is observed compared to AgNPs-EtOH. This could be explained by a better reduction of silver ions to elemental silver in the first case [42]. Moreover, the signals corresponding to other elements are much lower for AgNPs-H₂O, compared to AgNPs-EtOH. This could be explained by the presence of

phytochemical compound in higher amounts on the surface of AgNPs-EtOH compared to that of AgNPs-H₂O, taking into consideration that the plant's secondary metabolites act not only as reducing agents, but also as coating agents for AgNPs [43].

When analyzing the obtained TEM images, AgNPs-H₂O presented reduced dimensional uniformity. In contrast, AgNPs-EtOH had a more pronounced spherical shape than that of AgNPs-H₂O, and showed good dimensional uniformity, close to the average diameter of AgNPs-H₂O. Larger variations in the size and shape of AgNPs that were mentioned when detailing the obtained results may be due to the presence of different plant extract molecules found on the surface of nanoparticles [42]. This can be explained by the different parts of the plant taken into study (flowers vs. leaves), the different obtaining conditions for both the extract and the AgNPs, and, therefore, by a different chemical composition of the extract and, implicitly, of the AgNPs surface.

A larger size of AgNPs determined by DLS compared to TEM can be explained by the different principles of the two methods and by the fact that DLS measures the hydrodynamic size of AgNPs, which also includes the biomolecules found on the surface of nanoparticles.

In both cases, the obtained Zeta potential values are negative and relatively high, which contributes to the stabilization of the nanoparticles' dispersion in solvents, given the similar surface charge that leads to electrostatic repulsion between nanoparticles, thus preventing agglomeration. Researchers suggest that secondary metabolites present in the extract may be involved in the stabilization of AgNPs, which, in our case, can be represented by polyphenolic acids, flavonoids, carotenoids, and terpenes [44]. The Zeta potential of AgNPs-H₂O and of AgNPs-EtOH is similar to the value obtained by Padalia et al. (−27.63 mV) for AgNPs synthesized using an aqueous extract from *T. erecta* flowers [23].

2,2'-Azobis(2-amidinopropane) dihydrochloride (AAPH) has the ability to generate peroxy radicals and induce oxidative stress by affecting the cell and its subcellular structures. Peroxy radicals increase the rigidity of the red cell membrane and reduce its resistance. Studies in rats have shown the capacity of AAPH to induce hemolysis and to increase the number of carbonyl groups in proteins, thus, impairing tissue function. Peroxy radicals cause the oxidation of fatty acids found in the structure of phospholipid membranes and the reduction of erythrocyte resistance [45].

The ethanolic extract and the AgNPs obtained using the aqueous extract show the best capacity to block the prooxidant action of AAPH, thus, protecting erythrocytes against peroxy radicals. The protection induced by the ethanolic extract is close to that of gallic acid. The AgNPs synthesis increases the protective capacity of the aqueous extract from 48.48% (5 mg/mL) to 75.25% (5 mg/mL), but reduces that of the ethanolic extract by about five times, if considering EC₅₀ values. These variations could be determined by the different composition of the ethanolic and aqueous extracts, given the different solubility of natural compounds in the two used solvents.

A recent study carried out by Du et al. indicated the ability of peptides in brown rice extract to block the action of AAPH by reducing the hemolysis from 70% (in the absence of the extract) to a maximum of 20% (in the presence of the extract) [46]. All peptides analyzed contained tyrosine, therefore, the phenolic hydroxyl group may be considered to be involved in the AAPH neutralization process. Such groups are also present in the structure of polyphenols and flavonoids found in the extracts analyzed in this study.

The neutralization of peroxy radicals generated by AAPH is usually performed by compounds that possess hydrogen donor functional groups such as hydroxyl and carboxyl groups, but especially hydroxyl groups [47]. Polyphenols from plant extracts have the capacity of neutralizing peroxy radicals generated by AAPH, but at the same time, due to their ability to penetrate or attach to the hydrophilic region of the red cell membrane, can also slightly increase membrane fluidity and erythrocyte osmotic resistance, therefore, increasing the resistance to pro-oxidants [48].

Comparing the EC₅₀ values (µg/mL), the erythrocyte protection capacity of the analyzed samples decreases as follows: ethanolic extract (53.62 ± 1.96), AgNPs-H₂O

(70.83 ± 1.10), and AgNPs-EtOH (280.86 ± 0.89), the differences being statistically significant ($p < 0.01$).

Lipoxygenases catalyze the oxidation of unsaturated fatty acids to hydroperoxides which will initiate oxidation reactions affecting the structure of proteins, lipids, and nucleic acids. These oxidation reactions cause inflammatory phenomena, neurodegeneration, and deterioration of pathological conditions such as diabetes [49].

The lipoxygenase inhibition assay shows that the AgNPs obtained using the aqueous extract has a more intense action compared to the plant extract alone, the difference being statistically relevant ($p < 0.001$). Both the extracts and the nanoparticles have a lower action compared to gallic acid.

The increase in enzyme inhibition capacity observed in the case of AgNPs indicates the complexity of the enzyme-inhibitor interaction and their action directed to the active center of the enzyme, as well as it to its protein structure.

The inhibition of lipoxygenase is determined by both flavonoids and polyphenols present in plant extracts, the difference in activity being correlated with the chemical structure of these compounds. Both types of secondary metabolites are chemical constituents present in varying amounts in all plant extracts, which explains the ability of the extracts to block different forms of lipoxygenases [50].

The few previous studies conducted on various types of nanoparticles obtained using *T. erecta* extracts focus mostly on the characterization of the synthesized nanoparticles [22,24], with only some approaching the biological perspective of their potential use, especially as antimicrobials [23,25,26,51,52]. However, such studies were mostly conducted on extracts obtained from leaves and involved other types of nanoparticles as well. To the best of our knowledge, this is the first report on the evaluation of the antioxidant activity of AgNPs obtained using *T. erecta* flower extracts through the two chosen methods. One other previous study conducted on AgNPs obtained using *T. erecta* aqueous leaf extract assessed the antioxidant activity through DPPH scavenging assay, showing improved activity for the obtained nanoparticles compared to the initial extract [37].

Since antimicrobial resistance represents one of the most threatening health issues of the 21st century, the synthesis of effective antimicrobial agents proves to be very important, since many antibiotics have now become ineffective, as microorganisms continue to develop new mechanisms to resist their action [53]. Nanoparticles synthesized with the use of plants that show promising antimicrobial activity have high potential to be developed into future antibacterials and antifungals given their low toxicity [54].

AgNPs are known to be able to penetrate bacterial cell walls, producing changes in the structure of cell membranes and even leading to cell death. Their antibacterial properties are due to their nanoscale size, as well as to their large surface area to volume ratio. They can lead to an increase in cell membrane permeability, produce reactive oxygen species, and, through the release of silver ions, can interrupt the replication of DNA [55]. Furthermore, other factors can influence the antibacterial mechanisms of AgNPs such as the concentration of AgNPs, their shape and size, as well as the type of bacteria, with Gram-negative bacteria being more susceptible to their action compared to Gram-positive bacteria, taking into account the differences in cell wall structure [56].

The obtained values indicate that the biosynthesized AgNPs exhibit greater antifungal activity in comparison to the corresponding extract. The improved antifungal activity can be attributed to the small size of the AgNPs and to the presence of bioactive capping constituents. Small AgNPs can be easily diffused and could penetrate the fungal cell membrane and inhibit its growth by interfering with the usual biochemical processes. Moreover, active compounds from the plant extract that participate in the formation of AgNPs, such as polyphenols, organic acids, or flavonoids are also likely to be responsible for the synergistic effect that might generate the improved antifungal effect [8,57].

Our results are in partial agreement with previous studies conducted on different types of nanoparticles using *T. erecta* extracts (e.g., nickel oxide nanoparticles or silver nanoparticles obtained using leaf extracts, and zinc oxide nanoparticles using aqueous

extract of flowers) that showed a certain degree of inhibitory activity on Gram-positive and Gram-negative bacteria [25,51,58]. Regarding silver nanoparticles obtained from marigold flowers, one previous article investigated the synergistic potential of such nanoparticles when used with different commercial antibiotics, showing promising synergistic effects especially regarding antifungal activity [23].

5. Conclusions

The present work focused on completing a simple and eco-friendly green synthesis method of AgNPs with the use of two different *T. erecta* flower extracts. Our study provided evidence that the synthesized AgNPs represent promising candidates with potential use in future biomedical applications. The research implied the synthesis, characterization, and optimization of two types of nanoparticles using various modern techniques. FTIR and EDX analyses confirmed the presence of biocompounds surrounding the nanoparticles, while DLS studies showed that the size of AgNPs ranged from 104 to 123 nm. The in vitro antioxidant and antimicrobial activities assays carried out on the initial plant extracts and on their corresponding AgNPs showed that nanoparticles obtained using the aqueous extract presented improved antioxidant activity compared to the corresponding extract, while both types of AgNPs exhibited improved antifungal activity compared to the initial extracts.

Author Contributions: Conceptualization, A.F.B., M.H. and A.C.; formal analysis, A.F., S.R. and A.C.; investigation, A.F.B., I.M., C.M., A.F., I.-A.T.-M., C.T. and A.C.; methodology, M.H., C.M. and S.R.; software, I.-A.T.-M.; supervision, M.H. and A.C.; validation, A.F.; visualization, I.M., C.M. and C.T.; writing—original draft, A.F.B.; writing—review & editing, A.F.B., I.M. and A.C. All authors have read and agreed to the published version of the manuscript.

Funding: This research is part of a Young Researcher Grant, funded by “Grigore T. Popa” University of Medicine and Pharmacy, Iași, Romania, Grant Number 6984/21.04.2020”.

Institutional Review Board Statement: Not applicable.

Informed Consent Statement: Not applicable.

Conflicts of Interest: The authors declare no conflict of interest.

References

1. Ivănescu, B.; Burlec, A.F.; Crivoi, F.; Roșu, C.; Corciovă, A. Secondary metabolites from *Artemisia* genus as biopesticides and innovative nano-based application strategies. *Molecules* **2021**, *26*, 3061. [[CrossRef](#)]
2. Rai, S.; Rai, A. Review: Nanotechnology—The secret of fifth industrial revolution and the future of next generation. *Nusant. Biosci.* **2015**, *7*, 61–66. [[CrossRef](#)]
3. Abbasi, E.; Milani, M.; Fekri Aval, S.; Kouhi, M.; Akbarzadeh, A.; Tayefi Nasrabadi, H.; Nikasa, P.; Joo, S.W.; Hanifehpour, Y.; Nejadi-Koshki, K.; et al. Silver nanoparticles: Synthesis methods, bio-applications and properties. *Crit. Rev. Microbiol.* **2014**, *42*, 173–180. [[CrossRef](#)] [[PubMed](#)]
4. Wang, L.; Hu, C.; Shao, L. The antimicrobial activity of nanoparticles: Present situation and prospects for the future. *Int. J. Nanomed.* **2017**, *12*, 1227–1249. [[CrossRef](#)] [[PubMed](#)]
5. Bharathi, D.; Bhuvaneshwari, V. Evaluation of the cytotoxic and antioxidant activity of phyto-synthesized silver nanoparticles using *Cassia angustifolia* flowers. *Bionanoscience* **2019**, *9*, 155–163. [[CrossRef](#)]
6. Ansar, S.; Tabassum, H.; Aladwan, N.S.M.; Naiman Ali, M.; Almaarik, B.; AlMahrouqi, S.; Abudawood, M.; Banu, N.; Alsubki, R. Eco friendly silver nanoparticles synthesis by *Brassica oleracea* and its antibacterial, anticancer and antioxidant properties. *Sci. Rep.* **2020**, *10*, 18564. [[CrossRef](#)] [[PubMed](#)]
7. Khan, I.; Saeed, K.; Khan, I. Nanoparticles: Properties, applications and toxicities. *Arab. J. Chem.* **2019**, *12*, 908–931. [[CrossRef](#)]
8. Haghghi Pak, Z.; Abbaspour, H.; Karimi, N.; Fattahi, A. Eco-friendly synthesis and antimicrobial activity of silver nanoparticles using *Dracocephalum moldavica* seed extract. *Appl. Sci.* **2016**, *6*, 69. [[CrossRef](#)]
9. Burlec, A.F.; Pecio, L.; Kozachok, S.; Mircea, C.; Corciovă, A.; Verestiuc, L.; Cioancă, O.; Oleszek, W.; Hăncianu, M. Phytochemical profile, antioxidant activity, and cytotoxicity assessment of *Tagetes erecta* L. flowers. *Molecules* **2021**, *26*, 1201. [[CrossRef](#)] [[PubMed](#)]
10. Burlec, A.F.; Cioancă, O.; Mircea, C.; Arsene, C.; Tuchiluş, C.; Corciovă, A.; Hăncianu, M. Antioxidant and antimicrobial properties of *Chrysanthemum* and *Tagetes* selective extracts. *Farmacia* **2019**, *67*, 405–410. [[CrossRef](#)]
11. Neher, R.T. The ethnobotany of *Tagetes*. *Econ. Bot.* **1968**, *22*, 317–325. [[CrossRef](#)]
12. Lim, T.K. *Tagetes erecta*. In *Edible Medicinal and Non-Medicinal Plants*; Springer: Dordrecht, The Netherlands, 2014; pp. 432–447. ISBN 978-94-007-7394-3.

13. Maity, N.; Nema, N.K.; Abedy, M.K.; Sarkar, B.K.; Mukherjee, P.K. Exploring *Tagetes erecta* Linn flower for the elastase, hyaluronidase and MMP-1 inhibitory activity. *J. Ethnopharmacol.* **2011**, *137*, 1300–1305. [[CrossRef](#)]
14. Gong, Y.; Liu, X.; He, W.-H.; Xu, H.-G.; Yuan, F.; Gao, Y.-X. Investigation into the antioxidant activity and chemical composition of alcoholic extracts from defatted marigold (*Tagetes erecta* L.) residue. *Fitoterapia* **2012**, *83*, 481–489. [[CrossRef](#)] [[PubMed](#)]
15. Kaisoon, O.; Konczak, I.; Siriamornpun, S. Potential health enhancing properties of edible flowers from Thailand. *Food Res. Int.* **2012**, *46*, 563–571. [[CrossRef](#)]
16. Xu, L.; Chen, J.; Qi, H.; Shi, Y. Phytochemicals and their biological activities of plants in *Tagetes* L. *Chin. Herb. Med.* **2012**, *4*, 103–117. [[CrossRef](#)]
17. Pérez Gutiérrez, R.M.; Luna, H.H.; Garrido, S.H. Antioxidant activity of *Tagetes erecta* essential oil. *J. Chil. Chem. Soc.* **2006**, *51*, 883–886. [[CrossRef](#)]
18. Li, W.; Gao, Y.; Zhao, J.; Wang, Q. Phenolic, flavonoid, and lutein ester content and antioxidant activity of 11 cultivars of Chinese marigold. *J. Agric. Food Chem.* **2007**, *55*, 8478–8484. [[CrossRef](#)]
19. Barbieri, R.; Coppo, E.; Marchese, A.; Daglia, M.; Sobarzo-Sánchez, E.; Nabavi, S.F.; Nabavi, S.M. Phytochemicals for human disease: An update on plant-derived compounds antibacterial activity. *Microbiol. Res.* **2017**, *196*, 44–68. [[CrossRef](#)]
20. Dasgupta, N.; Ranjan, S.; Saha, P.; Jain, R.; Malhotra, S.; Saleh, M.A.A.M. Antibacterial activity of leaf extract of Mexican marigold (*Tagetes erecta*) against different Gram positive and Gram negative bacterial strains. *J. Pharm. Res.* **2012**, *5*, 4201–4203.
21. Giri, R.; Bose, A.; Mishra, S. Hepatoprotective activity of *Tagetes erecta* against carbon tetrachloride-induced hepatic damage in rats. *Acta Pol. Pharm. Drug Res.* **2011**, *68*, 999–1003.
22. Katta, V.K.M.; Dubey, R.S. Green synthesis of silver nanoparticles using *Tagetes erecta* plant and investigation of their structural, optical, chemical and morphological properties. *Mater. Today Proc.* **2021**, *45*, 794–798. [[CrossRef](#)]
23. Padalia, H.; Moteriya, P.; Chanda, S. Green synthesis of silver nanoparticles from marigold flower and its synergistic antimicrobial potential. *Arab. J. Chem.* **2015**, *8*, 732–741. [[CrossRef](#)]
24. Dhuldhaj, U.P.; Deshmukh, S.D.; Gade, A.K.; Yashpal, M.; Rai, M.K. *Tagetes erecta* mediated phytosynthesis of silver nanoparticles: An eco-friendly approach. *Nusant. Biosci.* **2012**, *4*, 109–112. [[CrossRef](#)]
25. Maji, A.; Beg, M.; Das, S.; Aktara, M.N.; Nayim, S.; Patra, A.; Islam, M.M.; Hossain, M. Study on the antibacterial activity and interaction with human serum albumin of *Tagetes erecta* inspired biogenic silver nanoparticles. *Process Biochem.* **2020**, *97*, 191–200. [[CrossRef](#)]
26. Navya Rani, M.; Murthy, M.; Shyla Shree, N.; Ananda, S.; Yogesh, S.; Dinesh, R. Cuprous oxide anchored reduced graphene oxide ceramic nanocomposite using *Tagetes erecta* flower extract and evaluation of its antibacterial activity and cytotoxicity. *Ceram. Int.* **2019**, *45*, 25020–25026. [[CrossRef](#)]
27. Singleton, V.L.; Rossi, J. Colorimetry of total phenolics with phosphomolybdic-phosphotungstic acid reagents. *Am. J. Enol. Vitic.* **1965**, *16*, 144–158.
28. Barros, L.; Falcão, S.; Baptista, P.; Freire, C.; Vilas-Boas, M.; Ferreira, I.C.F.R. Antioxidant activity of *Agaricus* sp. mushrooms by chemical, biochemical and electrochemical assays. *Food Chem.* **2008**, *111*, 61–66. [[CrossRef](#)]
29. Malterud, K.E.; Rydland, K.M. Inhibitors of 15-lipoxygenase from orange peel. *J. Agric. Food Chem.* **2000**, *48*, 5576–5580. [[CrossRef](#)]
30. CLSI. *Performance Standards for Antimicrobial Susceptibility Testing*, 30th ed.; CLSI supplement M100; Clinical and Laboratory Standards Institute: Wayne, PA, USA, 2020.
31. Clinical and Laboratory Standards Institute. M44-A2: Method for antifungal disk diffusion susceptibility testing of yeasts. In *Approved Guideline*, 2nd ed.; Clinical and Laboratory Standards Institute: Wayne, PA, USA, 2009.
32. Badi'ah, H.I.; Seede, F.; Supriyanto, G.; Zaidan, A.H. Synthesis of silver nanoparticles and the development in analysis method. *IOP Conf. Ser. Earth Environ. Sci.* **2019**, *217*, 012005. [[CrossRef](#)]
33. Shaheen, S.; Humma, Z.; Arooj, I.; Batool, S. Green synthesis of silver nanoparticles from flowers of *Helianthus annuus* and *Tagetes erecta* and their antibacterial activity against MDR pathogens. *RADS J. Biol. Res. Appl. Sci.* **2021**, *12*, 98–107. [[CrossRef](#)]
34. Kgatshe, M.; Aremu, O.S.; Katata-Seru, L.; Gopane, R. Characterization and antibacterial activity of biosynthesized silver nanoparticles using the ethanolic extract of *Pelargonium sidoides* DC. *J. Nanomater.* **2019**, *2019*, 3501234. [[CrossRef](#)]
35. Batir-Marin, D.; Mircea, C.; Boev, M.; Burlec, A.F.; Corciova, A.; Fifere, A.; Iacobescu, A.; Cioanca, O.; Verestiuc, L.; Hancianu, M. In vitro antioxidant, antitumor and photocatalytic activities of silver nanoparticles synthesized using *Equisetum* species: A green approach. *Molecules* **2021**, *26*, 7325. [[CrossRef](#)]
36. Siddiqi, K.S.; Husen, A.; Rao, R.A.K. A review on biosynthesis of silver nanoparticles and their biocidal properties. *J. Nanobiotechnol.* **2018**, *16*, 14. [[CrossRef](#)]
37. Tyagi, P.K.; Tyagi, S.; Gola, D.; Arya, A.; Ayatollahi, S.A.; Alshehri, M.M.; Sharifi-Rad, J. Ascorbic acid and polyphenols mediated green synthesis of silver nanoparticles from *Tagetes erecta* L. aqueous leaf extract and studied their antioxidant properties. *J. Nanomater.* **2021**, *2021*, 6515419. [[CrossRef](#)]
38. Corciova, A.; Ivanescu, B. Biosynthesis, characterization and therapeutic applications of plant-mediated silver nanoparticles. *J. Serbian Chem. Soc.* **2018**, *83*, 515–538. [[CrossRef](#)]
39. Siakavella, I.K.; Lamari, F.; Papoulis, D.; Orkoulas, M.; Gkolfi, P.; Lykouras, M.; Avgoustakis, K.; Hatziantoniou, S. Effect of plant extracts on the characteristics of silver nanoparticles for topical application. *Pharmaceutics* **2020**, *12*, 1244. [[CrossRef](#)]
40. Dias, A.C.P.; Marslin, G.; Selvakesavan, R.K.; Gregory, F.; Sarmiento, B. Antimicrobial activity of cream incorporated with silver nanoparticles biosynthesized from *Withania somnifera*. *Int. J. Nanomed.* **2015**, *10*, 5955. [[CrossRef](#)]

41. Mathur, P.; Jha, S.; Ramteke, S.; Jain, N.K. Pharmaceutical aspects of silver nanoparticles. *Artif. Cells Nanomed. Biotechnol.* **2018**, *46*, 115–126. [[CrossRef](#)]
42. Gaddam, S.A.; Kotakadi, V.S.; Subramanyam, G.K.; Penchalaneni, J.; Challagundla, V.N.; DVR, S.G.; Pasupuleti, V.R. Multifaceted phytogenic silver nanoparticles by an insectivorous plant *Drosera spatulata* Labill var. *bakoensis* and its potential therapeutic applications. *Sci. Rep.* **2021**, *11*, 21969. [[CrossRef](#)]
43. Kambale, E.K.; Nkanga, C.I.; Mutonkole, B.-P.I.; Bapolisi, A.M.; Tassa, D.O.; Liesse, J.-M.L.; Krause, R.W.M.; Memvanga, P.B. Green synthesis of antimicrobial silver nanoparticles using aqueous leaf extracts from three Congolese plant species (*Brillantaisia patula*, *Crossopteryx febrifuga* and *Senna siamea*). *Heliyon* **2020**, *6*, e04493. [[CrossRef](#)]
44. Shah, Z.; Hassan, S.; Shaheen, K.; Khan, S.A.; Gul, T.; Anwar, Y.; Al-shaeri, M.A.; Khan, M.; Khan, R.; Haleem, M.A.; et al. Synthesis of AgNPs coated with secondary metabolites of *Acacia nilotica*: An efficient antimicrobial and detoxification agent for environmental toxic organic pollutants. *Mater. Sci. Eng. C* **2020**, *111*, 110829. [[CrossRef](#)]
45. Gomes, D.; Carvalho, G.; Araujo, A.; Casquilho, N.; Valenca, S.; Leal-Cardoso, J.; Zin, W. 2,2'-azobis (2-amidinopropane) dihydrochloride (AAPH) impairs lung mechanics, morphology and oxidative balance in rats. *Eur. Respir. J.* **2014**, *44*, P2155.
46. Du, R.; Liu, K.; Zhao, S.; Chen, F. Changes in antioxidant activity of peptides identified from brown rice hydrolysates under different conditions and their protective effects against AAPH-induced oxidative stress in human erythrocytes. *ACS Omega* **2020**, *5*, 12751–12759. [[CrossRef](#)]
47. Barros, V.; Pereira, G.; Ota, S.; Melo, F.; de Jesus, A.C.; Lima, A.; da Silva, A.; Borges, R. A theoretical antioxidant mechanism for cytoprotective effect of p-acetamide-salicylate derivatives against free radical initiator AAPH in human erythrocytes. *J. Braz. Chem. Soc.* **2021**, *32*, 1354–1360. [[CrossRef](#)]
48. Cyboran-Mikołajczyk, S.; Kleszczyńska, H.; Oszmiański, J.; Paślowski, R. *Allium ursinum* L. leaves components modified the physico-chemical properties of red blood cells protecting them from the effects of oxidative stress. *Acta Pol. Pharm.-Drug Res.* **2019**, *76*, 483–491. [[CrossRef](#)]
49. Chedea, V.S.; Jisaka, M. Lipoygenase and carotenoids: A co-oxidation story. *Afr. J. Biotechnol.* **2013**, *12*, 2786–2791. [[CrossRef](#)]
50. Lončarić, M.; Strelec, I.; Moslavac, T.; Šubarić, D.; Pavić, V.; Molnar, M. Lipoygenase inhibition by plant extracts. *Biomolecules* **2021**, *11*, 152. [[CrossRef](#)] [[PubMed](#)]
51. Likasari, I.D.; Astuti, R.W.; Yahya, A.; Isnaini, N.; Purwiandono, G.; Hidayat, H.; Wicaksono, W.P.; Fatimah, I. NiO nanoparticles synthesized by using *Tagetes erecta* L. leaf extract and their activities for photocatalysis, electrochemical sensing, and antibacterial features. *Chem. Phys. Lett.* **2021**, *780*, 138914. [[CrossRef](#)]
52. Selvam, S.I.; Joicesky, S.M.B.; Dashli, A.A.; Vinothini, A.; Premkumar, K. Assessment of anti bacterial, anti inflammation and wound healing activity in Wistar albino rats using green silver nanoparticles synthesized from *Tagetes erecta* leaves. *J. Appl. Nat. Sci.* **2021**, *13*, 343–351. [[CrossRef](#)]
53. Dobrucka, R.; Długaszewska, J. Antimicrobial activities of silver nanoparticles synthesized by using water extract of *Arnicae anthodium*. *Indian J. Microbiol.* **2015**, *55*, 168–174. [[CrossRef](#)]
54. Teow, S.-Y.; Wong, M.; Yap, H.-Y.; Peh, S.-C.; Shameli, K. Bactericidal properties of plants-derived metal and metal oxide nanoparticles (NPs). *Molecules* **2018**, *23*, 1366. [[CrossRef](#)]
55. Yin, I.X.; Zhang, J.; Zhao, I.S.; Mei, M.L.; Li, Q.; Chu, C.H. The antibacterial mechanism of silver nanoparticles and its application in dentistry. *Int. J. Nanomed.* **2020**, *15*, 2555–2562. [[CrossRef](#)] [[PubMed](#)]
56. Loo, Y.Y.; Rukayadi, Y.; Nor-Khaizura, M.-A.-R.; Kuan, C.H.; Chieng, B.W.; Nishibuchi, M.; Radu, S. In vitro antimicrobial activity of green synthesized silver nanoparticles against selected Gram-negative foodborne pathogens. *Front. Microbiol.* **2018**, *9*, 1555. [[CrossRef](#)] [[PubMed](#)]
57. Teodoro, G.R.; Ellepola, K.; Seneviratne, C.J.; Koga-Ito, C.Y. Potential use of phenolic acids as anti-Candida agents: A review. *Front. Microbiol.* **2015**, *6*, 1420. [[CrossRef](#)] [[PubMed](#)]
58. Ilangovan, A.; Venkatraman, A.; Thangarajan, P.; Saravanan, A.; Rajendran, S.; Kaveri, K. Green synthesis of zinc oxide nanoparticles (ZnO NPs) using aqueous extract of *Tagetes erecta* flower and evaluation of its antioxidant, antimicrobial, and cytotoxic activities on HeLa cell line. *Curr. Biotechnol.* **2021**, *10*, 61–76. [[CrossRef](#)]